Technical University of Denmark

DTU

All-black front surfaces for building-integrated photovoltaics

Iandolo, Beniamino; Mizushima, Io; Davidsen, Rasmus Schmidt; Tang, Peter T.; Hansen, Ole

Link back to DTU Orbit

DTU Library
Technical Information Center of Denmark

All-black front surfaces for building-integrated photovoltaics

Beniamino Iandolo[1,*], Io Mizushima[2], Rasmus S. Davidsen[1], Peter T. Tang[2] and Ole Hansen[1]

[1]*DTU Nanotech, Technical University of Denmark, Kgs. Lyngby, DK-2800, Denmark*

[2]*IPU, Kgs. Lyngby, DK-2800, Denmark*

[*]E-mail: benian@nanotech.dtu.dk

Widespread implementation of building integrating photovoltaics requires aesthetically pleasant panels. Black surfaces are often visually appealing and, if based on a black photoabsorber, may lead to increased panel efficiency. Here, we demonstrate a combination of black silicon and black ribbons (or bus-bars), both fabricated with methods that are compatible with production lines of screen-printed, front contacted solar panels. Maskless, non-cryogenic reactive ion etch of silicon and subsequent coating with aluminum oxide for passivation purposes results in average reflectance of less than 1% in the UV-vis part of the solar spectrum, and in minority carrier lifetimes similar to those obtained on polished reference samples thanks to minimized surface damage, as confirmed by transmission electron microscopy. Inorganic blackening of bus-bars by a combination of electroplating and chemical etching results in reflectance values lower than 3.5% in the UV-vis, with no modifications to standard stringing equipment required.

1. Introduction

Developing aesthetically pleasant solar panels without excessive losses in power conversion efficiency is paramount to the broad diffusion of building-integrated photovoltaics[1–3]. A possible route, actually leading to *increased* efficiency, consists in replacing the standard wet textured silicon (obtained by alkaline and acidic texturing for mono- and multi-crystalline Si, respectively) with black silicon, which shows superior light trapping properties[4].

The expression black silicon (hereinafter b-Si), encompasses several types of nanostructured Si that exhibit strongly suppressed optical reflection at the Si-air interface[5]. A strong candidate for fabrication of b-Si is maskless, reactive ion etch (RIE)[6,7]. RIE can be used with success to texture any type of Si surface[8], and if performed at non-cryogenic temperatures[9] is readily compatible with existing production lines without dramatic increase in fabrication costs[10]. Furthermore, it does not suffer from metallic contamination as is the case for b-Si fabricated by metal assisted chemical etching (MACE), the other method of choice to obtain b-Si[11–13]. Finally, RIE offers a large parameter space for process tuning resulting in both ultra-low optical reflection and minimized surface charge carrier recombination[14]. Cell efficiencies of 22.1% and 21.9% have recently been reported for interdigitated back contact float-zone (FZ) Si and multi-crystalline Si respectively[15,16], with cryogenic RIE as front surface texturing. Also, cells with b-Si texturing are less affected by variation in incidence angle of light as compared to conventional textured cells[17], which is particularly relevant for building-integrated applications. Here, we have fabricated black Si by non-cryogenic RIE reaching the following targets: (i) average reflectance lower than 1% throughout the UV-vis part of the solar spectrum; and (ii) minority carrier lifetime values approaching those measured on polished Si wafers, as result of an optimized RIE process that leads to minimal surface damage.

Replacing wet textured Si with b-Si is clearly not the only modification required to improve the aesthetics of *front-contacted* panels, as sketched in Fig. 1. The current collecting strings, or bus-bars, display high reflectance in the visible due to their metallic nature (typically consisting of SnPbAg alloys). It follows that b-Si must be matched with bus-bars of similar appearance. Some bus-bars with dark appearance are commercialized. For example, Bruker-Spaleck produces solar ribbons with *organic* paint coating[18], while dark appearance ribbons with v-shaped structure invented by E. M. Sachs[19] are produced by Ulbrich[20]. Otherwise, few inorganic black bus-bars have been seen so far. In order to address this deficiency, we have developed a process for blackening bus-bars by combining metal coating by electroplating with chemical etching of the metal surface. The process is

compatible with large-volume industrial production and the coating is completely inorganic, thus expected to show excellent resistance to degradation by UV-light. Furthermore, the bus-bars are compatible with standard stringing equipment. Finally, they show reflectance of 4% or lower in the UV-vis range, thus matching the very low reflectance obtained by RIE-textured Si and making such a combination a very promising all-black front surface for standard processed solar cells.

2. Experimental methods

2.1 Fabrication of black silicon and lifetime samples.

100 mm diameter Czochralski (CZ) mono-crystalline (100) p-type doped Si wafers with thickness 350 ± 25 μm were textured using maskless RIE at -20 °C in a Pegasus system (STS) using the following parameters: gas flow ratio O_2: $SF_6 \approx 10$:7, chamber pressure of 4.5 Pa, coil power of 3000 W and platen power of 10 W or 60 W (both operating at 13.56 MHz radio-frequency), etching time 14 min. The wafers were then RCA cleaned, without the final oxide strip in hydrofluoric acid in order to leave on the surface the chemical oxide grown during RCA2. Subsequently, the wafers were coated with 380 cycles of Al_2O_3 synthesized at 200 °C using trimethyl-aluminum (TMA) and H_2O as precursors for Al and O, respectively, in an atomic layer deposition (ALD) process. These passivation layers were activated by post-deposition annealing for 10 min at 400 °C in a N_2 atmosphere using a Tempress furnace. For reference purposes, double-side polished wafers were also passivated and annealed.

2.2 Fabrication of black bus bars.

Both of electroplating and chemical etching of bus-bars were performed in a 1 L beaker at room temperature. The solutions were agitated with a magnetic stirrer. The bus-bars were degreased cathodically in an alkaline solution and pickled in a commercial acidic solution prior to the blackening process. After electroplating the bus-bars were rinsed with DI water, and immediately immersed in the chemical etching solution. Finally the bus-bars were with blow-dried using an air gun.

2.3 Characterization

The thickness of the Al_2O_3 layer was measured using ellipsometry (VASE J. A.Woollam Co.). Optical spectroscopy was performed in a UV spectrophotometer (UV-2600, Shimadzu Co.). Scanning electron microscopy (SEM) images were taken using a Carl Zeiss Supra 40VP

microscope at an acceleration voltage of 5 kV. Transmission electron microscope (TEM) images were acquired using a Titan 80-300 TEM microscope (FEI) at an accelerating voltage of 300 kV. Single nanostructures were isolated by pressing a Cu TEM grid with holey carbon on top of textured wafers. Effective lifetime measurements were performed using the microwave detected photoconductivity (MDP) method in transient and injection dependent single point mode, using a MDP mapper from Freiberg Instruments. In order to determine whether the blackened bus-bars were damaged upon stringing, cross-sections of bus-bars before and after soldering to a Si wafer were inspected using an optical microscope. For the observation a bus-bar and a piece of Si wafer with soldered bus-bar were mounted on epoxy resin separately, and the cross-sections were polished mechanically.

3. Results and discussion

3.1 Optical reflectance.

The first key metric to assess our procedures for suppressing reflection of light by Si and by the black bus-bars, clearly, is optical spectroscopy. Figure 2 summarizes the results of measurements of reflectance (R) in the wavelength range from 300 to 800 nm for b-Si and blackened bus-bars and compared to the reflectance of polished Si surfaces and of standard bus-bars obtained by soldering. After RIE texturing, the b-Si sample shows reflectance between 3 and 6% in the UV-A (300-400 nm wavelength), and lower than 3% throughout the visible spectrum. This is already lower reflectance than that of Si surfaces obtained by wet texturing[21,22]. Although RIE is capable of producing Si surfaces with yet lower reflectance[5], the reflectance obtained here is already low enough to relax requirements on thickness and composition of any anti reflective coating (ARC). This gives us an additional, useful handle to play with in terms of which material to choose for surface passivation (see also the following Subsection). We chose Al_2O_3 for this purpose, a material of proven performance thanks to its excellent chemical and physical passivation[23–25]. After depositing 35 nm of Al_2O_3 on top of our b-Si (thickness determined by ellipsometry and confirmed by TEM images, see next Subsection), we observed a further decrease in reflectance, such that R is lower than 1% throughout the visible spectrum, which brings the reflectance of our surfaces back on par with that of the structures described in Refs. 5, 17.

The reflectance of the bus-bars is also dramatically reduced by the blackening treatment. The standard bus-bars show reflectance values ranging from 30% at 300 nm to above 60% around 800 nm. After the blackening treatment, R is reduced to just 3.5% or less throughout the visible spectral range, matching very well the reflectance of our b-Si.

3.2 Morphology and lifetime of passivated b-Si.

Figure 3(a)-(b) show top-view and cross-section SEM images of a wafer textured by our RIE process, respectively. The nanostructures appear as randomly distributed hillocks, with shape generally varying between that of a cone and that of a paraboloid[14]. The base of the nanostructures has a characteristic dimension between 200 and 300 nm, and a maximum height of about 500 nm. The Al_2O_3 coating shows excellent degree of conformity, as expected from ALD[26]. The uniformity of the RIE processing can be appreciated from Fig. 3(c), which contains a photograph of a 100 mm diameter wafer after RIE. Figure 3(d) summarizes effective lifetime measurements on our b-Si and polished reference sample. The effective lifetime of b-Si before passivation is rather low and at most of 10 μs, as common for non-passivated Si surfaces[27]. The lifetime is improved by deposition of Al_2O_3, and reaches about 50 μs. A further improvement of a factor of more than 20 is observed upon annealing of Al_2O_3 in N_2 ambient at 400 °C for 10 minutes. The need for annealing (usually at temperatures between 350 °C and 500 °C, in N_2 or forming gas) to activate the passivation effect of Al_2O_3 is well-known in the literature[27]. In our b-Si case, the highest measured effective lifetime is 1.17 ms, not far from the highest lifetime obtained on the passivated, polished Si reference sample (1.54 ms). This proves that our RIE process is rather gentle and does not damage the Si surface critically.

TEM characterization of nanostructures obtained using different RIE parameters can help elucidating the promising results in terms of effective lifetime. Figure 4(a)-(b) show low magnification TEM images of single nanostructures fabricated using a high RIE platen power (60 W) and a low RIE platen power (10 W), respectively. It is clear that the Al_2O_3 coating is conformal in both cases. High resolution TEM (HRTEM) imaging, however, reveals a clear difference in the quality of the Si/Al_2O_3 interface. This is crucial for surface recombination[25], since a low quality interface may worsen both the chemical passivation (i.e., how dangling bonds in Si are satisfied) and the physical passivation (since it is due to the sheet charge in close proximity of the interface). In the case of high RIE platen power (Fig. 4(c)), we can identify a region of a few nm in thickness, in which the Si appears to have become amorphous. This is most likely a result of the higher energy and more intense ion bombardment during RIE caused by the higher platen power. On the other hand, in the case of low RIE platen power (Fig. 4(d)) the lattice planes of Si with a distance of 3.13 Å are readily identified, corresponding to the (111) set of planes. These atomic columns of Si extend all the way to the boundary with Al_2O_3 without visible damage, which indicates an

interface of high quality where the Al_2O_3 passivation properties are fully exploited.

3.3 Black bus-bars.

The surface of blackened bus-bar is shown in the SEM image of Fig. 5(a). Some holes in the coating are visible with characteristic dimensions of around 1 μm, which however do not affect the functionality and the antireflective properties of the coating. In fact, the coating reduces reflectance dramatically as compared to conventional bus-bars with soldering coating, as already discussed in Section 3.1. Figure 5(b)-(c) show cross-sections of bus-bars before and after stringing, respectively. The soldering coating on the top side does not change during soldering, while some solder material on the back Si is redistributed due to surface tension. Chemical analysis by energy dispersive X-rays spectroscopy (data not shown here) shows that the coating on the top side has not been damaged by the soldering process or the flux that was used before soldering. The small hole in the top layer on Fig. 5(c) (indicated by the white circle) was caused by one of the pins from the stringer-machine during soldering. However, such hole is not visible from a distance of 1 m. In addition, one can notice a few small imperfections between cell and bus-bar. However, these imperfections in the soldering are not caused by the blackening of the bus-bars, as confirmed by analysis of several cross-sections after using the same stringing machine, including standard, non-blackened bus-bars, which all contained similar minute imperfections.

4. Conclusions

In this paper, we have introduced black silicon textured by maskless, non-cryogenic reactive ion etch together with black bus-bars towards aesthetically appealing screen-printed, front contacted solar panels. Black silicon coated with Al_2O_3 results in a uniform dark appearance with average reflectivity lower than 1% in the UV-vis part of the solar spectrum, while retaining good minority carrier effective lifetime (up to 1.14 ms as compared to 1.54 ms for planar, polished reference wafers). The relatively high effective lifetime of black silicon samples is ascribed to a lower surface and sub-surface damage in the silicon thanks to the lower ion energy during the etching process, as revealed by high resolution transmission electron microscopy analysis. Blackened bus-bars using inorganic treatment combining electroplating and chemical etching results in reflectance lower than 4% across the UV-vis range, matching the antireflective properties of the black silicon rather well. Current efforts are being devoted to incorporating both black-Si and black bus-bars in a pilot production line of front-contacted panels, while future work will focus on up-scaling the blackening

process for the bus-bars to an automated line fabricating selective blackening at high speeds. In addition, we have planned accelerated ageing tests on mini-modules in order to assess the reliability and performance over time of our all-black panels.

Acknowledgments

References

(1)   S. S. Chicago, S. Hogan, Photovoltaics Bull., **9**, 7-9 (2003).

(2)   P. B. Rand, J. Genoe, P. Heremans, J. Poortmans, Prog. Photovolt Res. Appl., **15**, 659-676 (2007).

(3)   C. Peng, Y. Huang, Z. Wu, Energy Build., **12**, 3592–3598 (2011).

(4)   X. Liu, P. R. Coxon, M. Peters, B. Hoex, J. M. Cole, D. J. Fray, Energy Environ. Sci., **7**, 3223-3263 (2014).

(5)   K. Füchsel, M. Kroll, M. Otto, M. Steglich, A. Bingel, T. Käsebier, R. B. Wehrspohn, E. B. Kley, T. Pertsch, A. Tünnermann, Proc. of SPIE, **8438**, 117–151 (2012).

(6)   H. Jansen, M. De Boer, R. Legtenberg, M. Elwenspoek, J. Micromechanics Microengineering, **2**, 115–120 (1995).

(7)   J. S., Yoo, L. O. Parm, U. Gangopadhyay, K. Kim, S. K. Dhungel, D. Mangalaraj, J. Yi, Sol. Energy Mater. Sol. Cells, **90**, 3085-3093 (2006**).

(8)   B. Kafle, T. Freund, A. Mannan, L. Clochard, E. Duffy, S. Werner, P. Saint-Cast, M. Hofmann, J. Rentsch, R. Preu, Energy Procedia, **92**, 359-368 (2016).

(9)   R. S. Davidsen *et. al.*, Sol. Energy Mater. Sol. Cells, **144**, 740–747 (2016).

(10)   B. Kafle, A. Mannan, T. Freund, L. Clochard, E. Duffy, M. Hofmann, J. Rentsch, R. Preu, Phys. Status Solidi - Rapid Res. Lett., **9**, 448–452 (2015).

(11)   J. Oh, H. C. Yuan, H. M. Branz, Nat. Nanotechnol. **7**, 743–748 (2012).

(12)   X. Li, Y. Xiao, C. Yan, K. Zhou, S. L. Schweizer, A. Sprafke, J.-H. Lee, R. B. Wehrspohn, ECS Solid State Lett., **2**, 22-24 (2012).

(13)   M. Algasinger, J. Paye, F. Werner, J. Schmidt, M. S. Brandt, M. Stutzmann, S. Koynov, Adv. Energy Mater., **3**, 1068-1074 (2013).

(14)   M. M. Plakhotnyuk, M Gaudig, R. S. Davidsen, J. M. Lindhard, J. Hirsch, D. Lausch, M. S. Schmidt, E. Stamate, O. Hansen, J. Appl. Phys., **122**, 143101 (2017).

(15)   H. Savin, P. Repo, G. Von Gastrow, P. Ortega, E. Calle, M. Garín, R. Alcubilla, Nat. Nanotechnol.**, 10,** 624-628 (2015).

(16) F. Schindler, B. Michl, P. Krenckel, S. Riepe, J. Benick, R. Müller, A. Richter, S. W. Glunz, M. C. Schubert, Energy Procedia, **124**, 777–780 (2017).

(17) R. S. Davidsen, J. Ormstrup, M. L. Ommen, P. E. Larsen, M. S. Schmidt, A. Boisen, Ø Nordseth, O. Hansen, Sol. Energy Mater. Sol. Cells, **140**, 134–140 (2015).

(18) Solar Ribbon for Photovoltaic Modules, http://www.bruker-spaleck.com/en/products/solarband-fuer-photovoltaikmodule-en.

(19) Sachs, E. M. Light Capture with Patterned Solar Cell Bus Wires, US patent (2007**)**.

(20) Light Capturing Ribbon, https://www.pvribbon.com/.

(21) S. W. Park, J. Kim, S. Lee, Application of Acid Texturing to Multi-Crystalline Silicon Wafers. J. Korean Phys. Soc., **43**, 423-426 (2003).

(22) K. Kim, S. K. Dhungel, S. Jung, D. Mangalaraj, J. Yi, J. *Sol. Energy Mater. Sol. Cells*, **92**, 960–968 (2008).

(23) B. Hoex, J. J. H. Gielis, M. C. M. Van De Sanden, W. M. M. Kessels, J. Appl. Phys., 104, 113703 (2008).

(24) B. Hoex, M. C. M. van de Sanden, J. Schmidt, R. Brendel, W. M. M. Kessels, Phys. Status Solidi - Rapid Res. Lett., **6**, 4-6 (2012).

(25) G. Dingemans, W. M. M. Kessels, J. Vac. Sci. Technol. A Vacuum, Surfaces, Film*, **30***, 40802*, (2012).

(26) S. M. George, Chem. Rev., **110**, 111–131 (2010).

(27) A. Cuevas, D. Macdonald, Sol. Energy, **76**, 255–262 (2004).

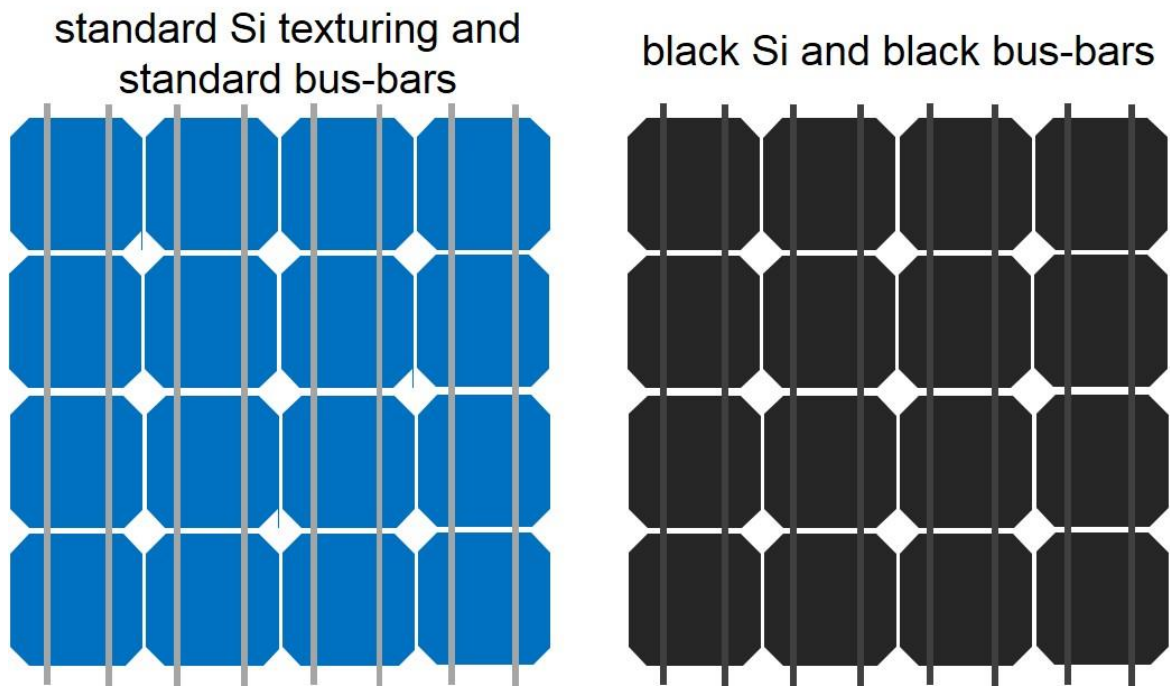**Fig. 1.** (Color online). Schematic of front contacted standard cells compared to cells with black silicon and black bus-bars.
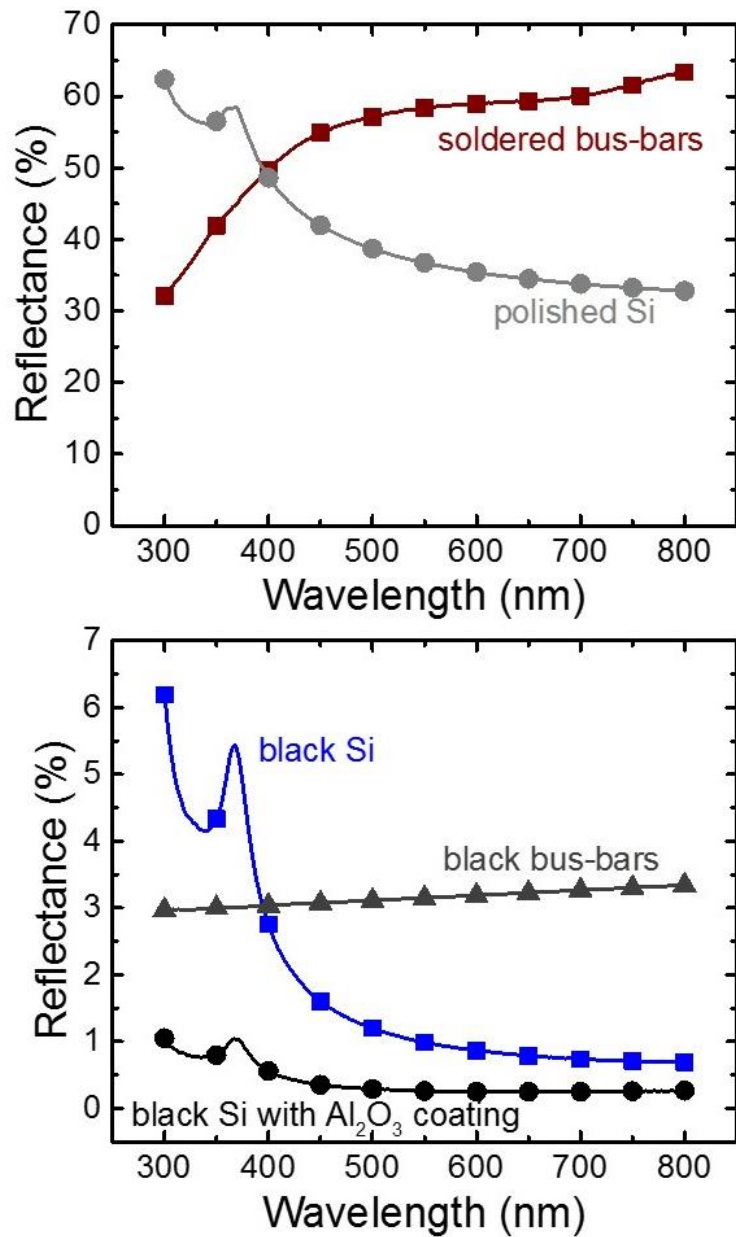
Fig. 2. (Color online). Top: reflectance as function of photon wavelength for CZ, p-type polished Si (circles) and for standard bus-bars (squares). Bottom: reflectance as function of photon wavelength for b-Si after RIE (squares) and after deposition of ALD Al_2O_3 (circles), as well as for and blackened bus-bars (triangles).
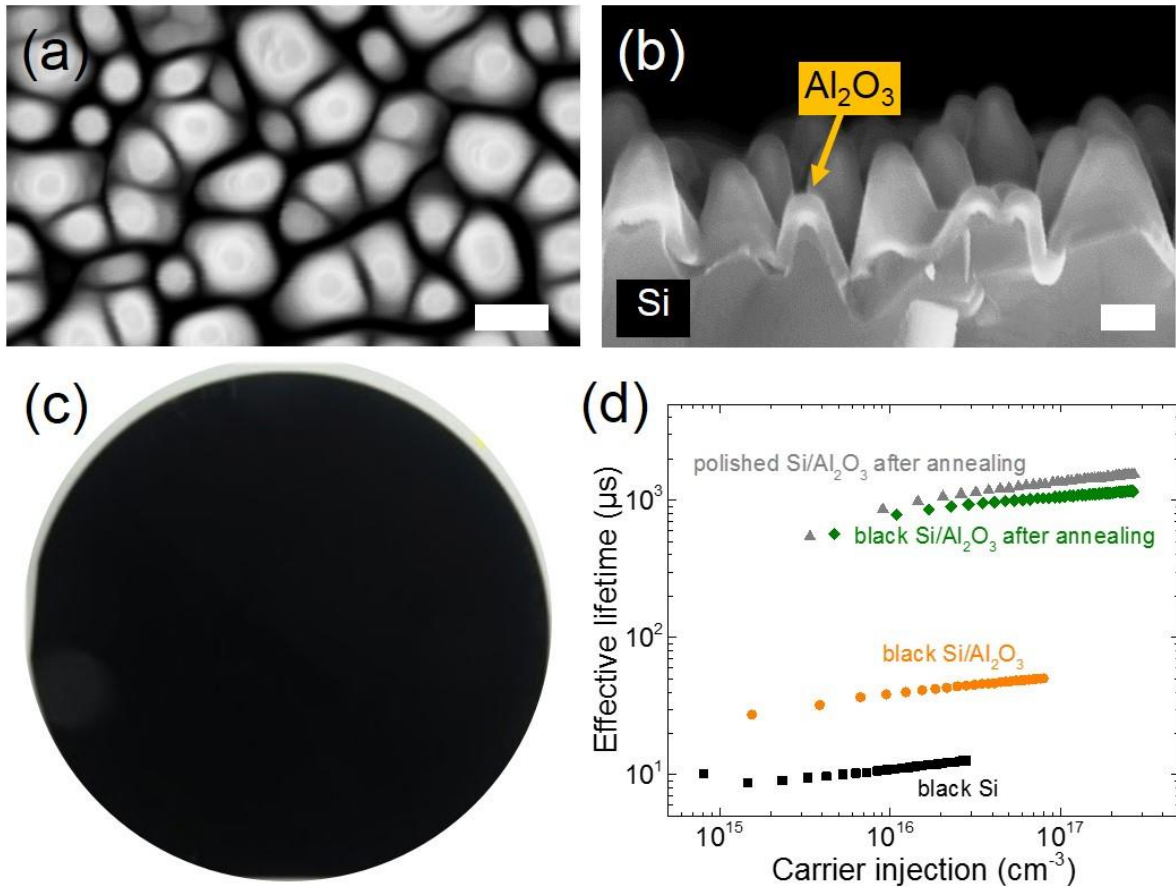
Fig. 3. (Color online). (a) Top-view SEM image of b-Si passivated with ALD Al$_2$O$_3$. Scale bar is 200 nm. (b) Cross-section SEM image of b-Si passivated with ALD Al$_2$O$_3$. Scale bar is 100 nm. (c) Photograph of a 4'' p-type CZ wafer after texturing with RIE, showing excellent uniformity in the etching process. (d) Effective lifetime measurements on b-Si before passivation (squares), after passivation (circles), and after annealing (diamonds). The effective lifetime of a polished CZ p-type wafer after passivation and annealing is also shown for reference.
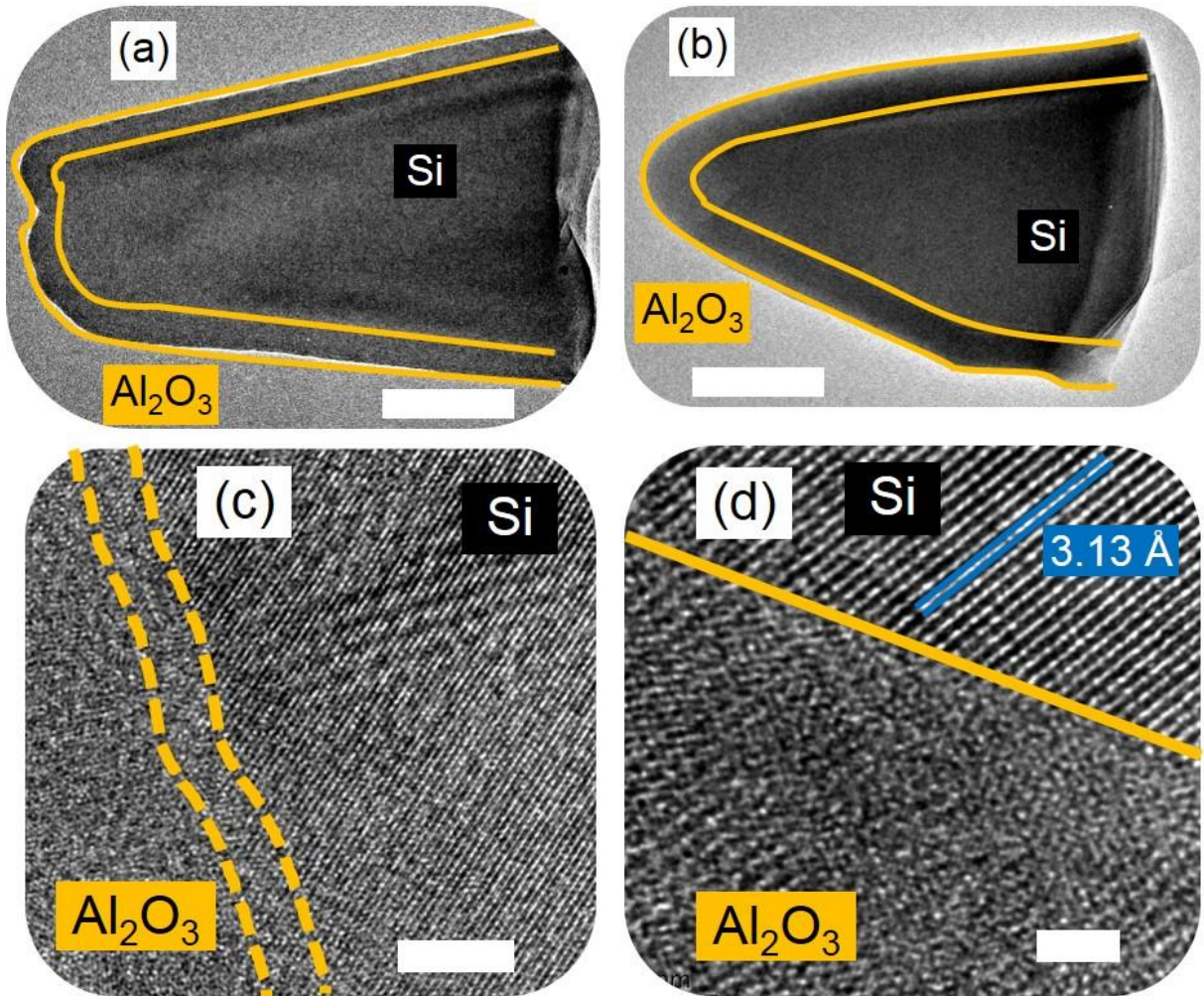
Fig. 4. (Color online). TEM characterization of nanostructures from b-Si. (a) TEM image of a single nanostructure resulting from high surface damage RIE processing. The yellow contours indicate the Al_2O_3 passivation layer deposited by ALD. The scale bar is 100 nm. (b) TEM image of a single nanostructure resulting from low surface damage RIE processing (i.e. same wafers used for lifetime measurements shown in Fig. 3(d)). The yellow contours indicate the Al_2O_3 passivation layer deposited by ALD. The scale bar is 100 nm. (c) HRTEM image of the Si/Al_2O_3 interface in the nanostructure shown in (a). The interface is not clear and a region of disorder (with possibly amorphized Si) is visible. Scale bar is 5 nm. (d) HRTEM image of the Si/Al_2O_3 interface in the nanostructure shown in (b). A much clearer interface is visible. The atomic columns of Si extend all the way to the interface (the distance between planes is 3.13 Å, corresponding to the (111) set of planes. Scale bar is 2 nm
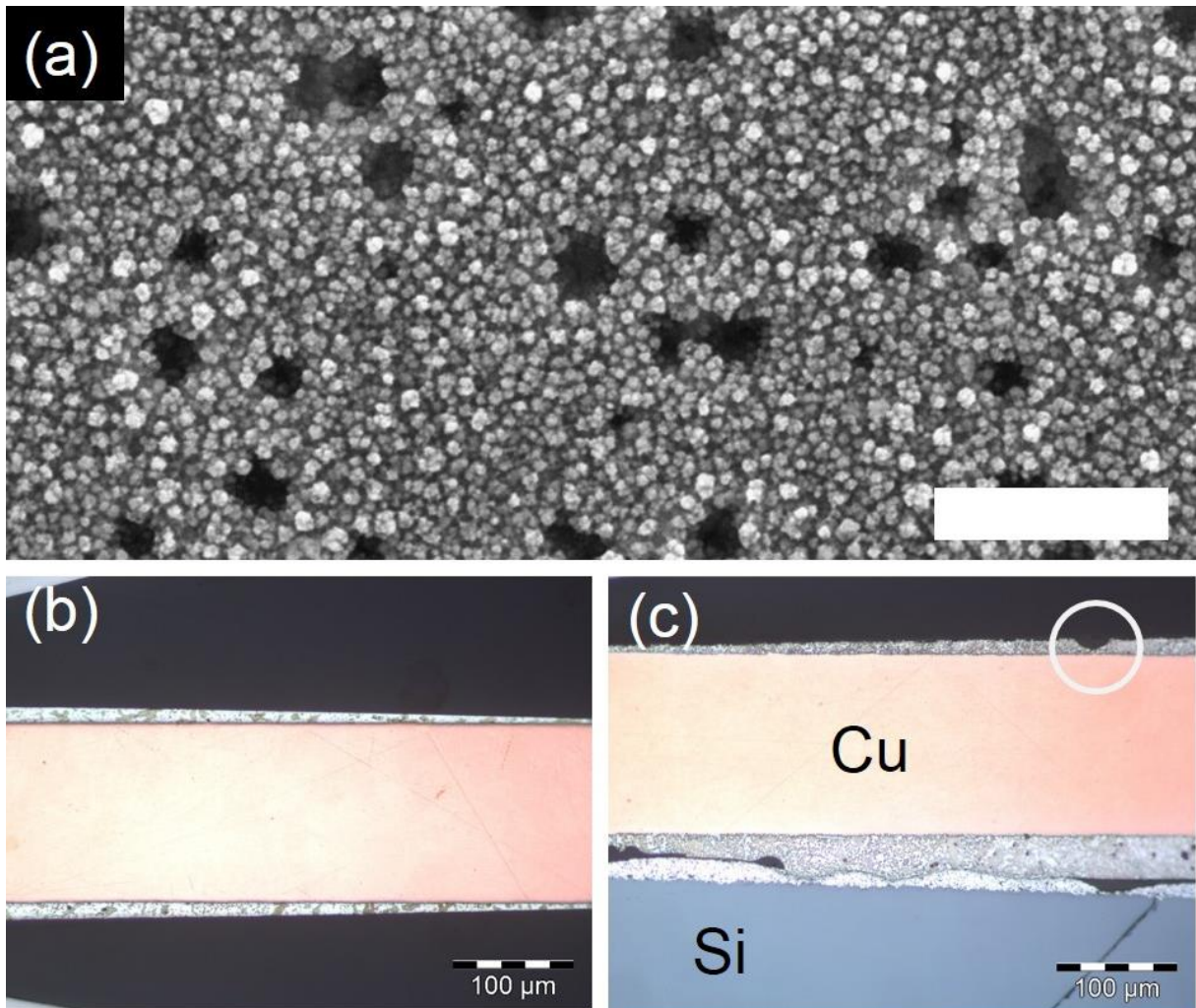
Fig. 5. (Color online). (a). Top-view SEM image of surface of blackened bus-bar. Scale bar is 5 μm. (b) Optical microscope of a polished cross-section of blackened bus-bars before stringing. (c) Optical microscope of a polished cross-section of blackened bus-bars after stringing. The white circle indicates a small hole caused by a pin during the stringing process, which however is not visible from a distance of 1 m.